J Neurophysiol 101: 843–854, 2009.
First published December 10, 2008; doi:10.1152/jn.90679.2008.

Neuromechanics of Muscle Synergies During Cycling

James M. Wakeling[1] and Tamara Horn[2]

[1]*School of Kinesiology, Simon Fraser University, Burnaby, British Columbia, Canada; and* [2]*Swiss Federal Institute of Technology, Zurich, Switzerland*

Submitted 13 June 2008; accepted in final form 28 November 2008

Wakeling JM, Horn T. Neuromechanics of muscle synergies during cycling. *J Neurophysiol* 101: 843–854, 2009. First published December 10, 2008; doi:10.1152/jn.90679.2008. Muscle synergies have been proposed as building blocks that could simplify the construction of motor behaviors. However, the muscles within synergistic groups may have different architectures, mechanical linkages to the skeleton, and biochemical properties, and these put competing demands on the most appropriate way to activate them for different mechanical tasks. This study identifies the extent to which synergistic patterns of muscle activity vary when the mechanical demands on a limb were altered, and additionally identifies how consistent the spectral profiles of the electromyographic (EMG) intensities were across the different movement tasks. The muscle activities were measured with surface EMG across 10 muscles in the leg during cycling at a range of loads and velocities. The EMGs were quantified by their intensities in time-frequency space using wavelet analysis; the instantaneous patterns of activity identified using principal component analysis, statistically compared and further visualized using the varimax rotation. Variability (35.7%) in the patterns of activity between the muscles were correlated with the torque and velocity of the pedal crank. Anatomic groups of muscles share a common mechanical action across a joint; uncoupling between such muscles was identified in 68.8% of the varimax patterns that encompassed all 10 muscles and 20.8–29.5% of the activity patterns when the anatomic groups were analyzed separately. The EMG spectra showed greatest heterogeneity for the gastrocnemii. These results show that the activity of muscles within anatomic groups is partially uncoupled in response to altered mechanical demands on the limb.

INTRODUCTION

Movements are achieved by the concerted action of the many muscles throughout the body. The muscles act to not only produce or dissipate the work required for each movement but also to redistribute that work among the different body segments (Zajac et al. 2002). Thus many muscles may be necessary for a coordinated motion even if their primary functions do not appear to power that movement. The question of how the CNS coordinates activity between different muscles is central to an understanding of motor control.

Muscle synergies have been described as coherent activations, in space or time, of groups of muscles (d'Avella and Bizzi 2005). These synergies can simplify the coordination of complex movements with the resultant activation of a set of muscles being derived from a combination of synergies that is appropriate to the movement behavior. Muscle synergies for groups of 7–16 muscles have been described for a range of activities. The kinematics (direction) of hindlimb kicking in frogs has been related to a set of three time-varying muscle synergies (d'Avella et al. 2003). Four main muscle synergies are used by the cat for postural corrections in response to lateral perturbations and the level of synergies activated is related to the direction of the perturbation (Ting and Macpherson 2005). In man, five synergies have been shown to control $\leq$16 different muscles during walking at a range of speeds and gravitational loads (Ivanenko et al. 2004). Simulation studies have predicted that six muscle synergies can robustly explain forward pedalling (Raasch and Zajac 1999), and observations show that backward pedalling can be achieved with similar synergies if the synergy responsible for changes in anterior/posterior pedal direction is reversed in its timing (Ting et al. 1999). Basic muscle synergies are shared across different locomotor behaviors, as demonstrated between swimming, walking and jumping in the frog (d'Avella and Bizzi 2005). A common feature that has been identified about muscle synergies is that they are related to the position of the limb during a gait cycle (Raasch and Zajac 1999; Ting et al. 1999) or to the direction of the movement (d'Avella et al. 2003; Ting and Macpherson 2005); and so muscle synergies have been proposed as building blocks that could simplify the construction of motor behaviors (d'Avella et al. 2003).

The function of individual muscles is largely determined by their architecture (Lieber and Fridén 2000), moment arms, and fiber-type composition (Rome et al. 1988). As the pennation angle increases, the physiological cross-sectional area (area perpendicular to the fiber direction) will increase and is typically accompanied by a decrease in the ratio of the muscle fiber length to the whole muscle length; these changes predispose the muscle to generate greater forces with reduced fascicle strains (Lieber and Fridén 2000). Increases in the moment arm between the muscle and joint result in increases in muscle strain and strain rate for a given joint motion (Rome et al. 1988); correspondingly, if a muscle inserts further away from a joint, it will generate greater joint torques but move the joint through a smaller range of motion and velocity for a given muscle contraction (Hildebrand and Goslow 2001). In this study, we use the term anatomic groups to refer to muscles that share a common mechanical action across a joint. The preceding arguments predict that when muscles from the same anatomic group have different moment arms they will be better suited to different mechanical tasks. Different muscle fiber types have optimal contraction speeds at different velocities (strain rates), and so faster muscle may be suited to faster movements (Rome et al. 1988). Muscles from an anatomic group may have varied architectural and fiber-type properties and so should be expected to contribute differently to movements with different mechanical demands. For instance, within the ankle extensor

Address for reprint requests and other correspondence: J. M. Wakeling, Department of Biomedical Physiology and Kinesiology, Simon Fraser University, Burnaby, BC V5A 1S6, Canada

The costs of publication of this article were defrayed in part by the payment of page charges. The article must therefore be hereby marked "*advertisement*" in accordance with 18 U.S.C. Section 1734 solely to indicate this fact.

0022-3077/09 $8.00 Copyright © 2009 The American Physiological Society

Downloaded from http://jn.physiology.org/ by 10.220.33.3 on November 11, 2017

group, the soleus muscle has a greater proportion of slow muscle fibers (Johnson et al. 1973) and has a lower fiber to muscle length ratio (Lieber and Fridén 2000; Wickiewicz et al. 1983) than either the lateral or medial gastrocnemius. It has been shown that the muscle activity in the soleus and medial gastrocnemius in the cat both increase with increased intensities of locomotion (Kaya et al. 2003), but during the paw-shake (which is a high-frequency contraction), the activity in the medial gastrocnemius is large, but it is virtually absent in the soleus (Smith and Spector 1981; Smith et al. 1980); thus the relative activity found between these muscles during walking can be uncoupled for the different mechanical function of the paw shake. Similar results have been reported in man where the gastrocnemii are used more for higher speed contractions and the soleus for higher load contractions during cycling (Wakeling et al. 2006).

For an animal to perform a range of behaviors, its limbs are required to move in a controlled fashion at a wide range of velocities and loads. One study to investigate how muscle synergies adapt to a range of locomotor speeds quantified the synergies from $\leq$16 muscles during walking and running between 1 and 5 m s^{-1} in man (Ivanenko et al. 2004). The EMG recordings were initially normalized for each condition before factor analysis was used to determine muscle synergies. This approach meant that the synergies did not reflect the absolute levels of EMG or the relative changes in EMG between the muscles; however, it was reported that the activation patterns of individual muscles varied dramatically with speed (Ivanenko et al. 2004). The muscle synergy arguments for coherently recruiting muscles together is different from the architectural and fiber-type (anatomic group) arguments that suggest that muscles may be best used independently. Clearly, muscle synergies and patterns of motor control must adapt to the velocity of the locomotor task and this could potentially occur with the introduction of new synergies or the modulation of already active synergies. However, the effect of velocity has not been determined for muscle synergies.

The purposes of this study were first, to determine the extent to which the patterns of activity across a range of muscles in the leg are modulated by the mechanics of the movement. The term pattern of activity is used to refer to the relative levels of activation that can occur across a set of muscles at a set moment in time. A pattern of activation may correspond to a muscle synergy that is a component of the task, and it may refer to synergy that has been modulated by feedback: we cannot distinguish between these two cases in this study and so use the term pattern of activity rather than synergy. If the muscle synergies were determined purely by the locomotor behavior (i.e., walking or cycling), then the patterns of activity would be governed by kinematic position (that is related to the crank angle during cycling) and not to the velocity or load of the task. However, here we hypothesized that a significant (>10%) proportion of the patterns of activity are modulated due to the movement mechanics (the load and velocity required during the task). The second purpose was to test the hypothesis that activity of muscles within an anatomic group would show a significant (>10%) uncoupling when the limb was challenged with a range of mechanical conditions. An additional aim of the study was to characterize the time-varying spectral properties of the leg muscles during these cycling tasks to compliment previously reported data from the triceps surae muscles (Wakeling et al. 2006).

METHODS

Approach to the problem

To relate changes in patterns of muscle activation with changes in load and speed, it is necessary to minimize other potential confounding effects such as altered gait kinematics, stability control, or weight support. Increases in velocity during walking and running typically involve increases in (ground reaction) forces, making it difficult to experimentally uncouple load and velocity. Pedalling on a stationary cycle ergometer provides a good experimental model for studying the effect of varying locomotor load and velocity on the motor control patterns because the kinematics are constrained to one pedalling gait, the muscle coordination patterns applicable to propulsion should dominate, and load and velocity can be independently varied. To minimize any possible bias to the EMG signals that can occur with changes in muscle temperature or fatigue, the subjects were required to warm up before testing, and the experimental conditions were presented in a randomized block fashion. The fastest pedal rates (140 revolution/min, rpm) are challenging or even impossible for untrained cyclists, and so it was necessary to recruit experienced cyclists so that a wide range of mechanical conditions could be tested.

Muscle synergies can be quantified by the time-varying patterns of the levels of EMG across groups of muscles and a number of different matrix factorization algorithms have previously been used to determine muscle synergies (Tresch et al. 2006). A common feature of all factor analyses is that each factor does not necessarily resemble the actual levels of activity present in each muscle, instead the measured activity patterns are represented by the vector products of the factors (principal component, PC weightings) and their loading scores. For instance, the first PC explains the largest source of variation in the set of muscle activity patterns and typically resembles the mean activity pattern across the set; on average all the muscles are active to some degree and so the first PC weighting shows a contribution of every muscle. This does not imply that all muscles were active simultaneously because the actual activity patterns measured additionally have contributions (both positive and negative) from the other PCs. The interpretation of the PCs can be simplified by using a varimax rotation to minimize the number of variables with high loadings on each component (Ivaneko et al. 2004; Kaiser 1958). These rotated components are more similar to those of the muscle activity patterns than the PCs (Chau 2001; Davis and Vaughan 1993). In this study, we use principal component analysis to characterize the EMG signals. The identified factors are similar to the muscle synergies described in previous studies (Ivaneko et al. 2004; Tresch et al. 2006), but here we refer to them as patterns of activity because the experimental protocol may result in them describing both synergies and the modulations to those synergies that occur with altered movement mechanics.

Cycling

Nine male cyclists (age 33.9 ± 2.9 yr; mass: 76.1 ± 4.4 kg; height: 1.79 ± 0.02 m: means ± SE) were tested at the Neuromuscular Mechanics Laboratory, School of Kinesiology, Simon Fraser University. Subjects gave their informed consent in accordance with the SFU Office of Research Ethics approval. The subjects were club to national level racing cyclists.

Subjects cycled with clipless pedals on a stationary dynomometer (SRM indoor trainer, Schoberer Rad Meβtechnik, Jülich, Germany), equipped with torque sensing cranks (SRM Powermeter). Subjects initially cycled at a low power for 5 min to get accustomed to the dynomometer, and then data were recorded for nine experimental conditions presented three times in a randomized block format. Data were recorded for 30 s of steady cycling for each condition, and a rest of 45 s was given between conditions. The test conditions were: 60, 80, 100, 120, or 140 rpm at a crank torque of 6.5 N m and additionally crank torques of 12.9, 25.1, 32.4, and 39.9 N m at a pedal cadence of 60 rpm.

Downloaded from http://jn.physiology.org/ by 10.220.33.3 on November 11, 2017

Bipolar Ag/AgCl surface EMG electrodes (10 mm diam, 21 mm interelectrode distance) were placed in the center of the muscle bellies of the tibialis anterior (TA), medial gastrocnemius (MG), lateral gastrocnemius (LG), soleus (Sol), vastus medialis (VM), rectus femoris (RF), vastus lateralis (VL), biceps femoris long head (BF), semitendinosus (ST), and gluteus maximus (GM) on the left leg after prior removal of the hair and cleaning with isopropyl wipes. EMG signals were amplified (Biovision, Wehrheim, Germany) and recorded at 2,000 Hz via a 16-bit A/D convertor (USB-6210, National Instruments, Austin, TX). Heart rate was monitored using a T31 transmitter and wireless receiver (Polar Electro Canada), and the pedal position was determined once per cycle via a magnetic pedal switch that was activated when the left pedal crank was nearly vertically up: these data were recorded simultaneously with the EMG. The crank power (mechanical power required to turn the cranks) was sampled at 1 Hz and monitored and recorded on a separate computer using SRMWin software, and the mean crank power and torque calculated for trial.

Data analysis

The myoelectric signals were resolved into their EMG intensities in time-frequency space using wavelet techniques (von Tscharner 2000). The total EMG intensity at each time point was calculated across the frequency band (11–432 Hz) and is a measure of the time-varying power within the signal. The total EMG intensity is a positive envelope quantifying the EMG and is equivalent to twice the square of the root-mean-square of the EMG; the time resolution for determining the EMG intensity was ~20 ms for frequencies >100 Hz. The EMG intensity spectrum is equivalent to the power spectrum from the EMG signal. The total EMG intensity and the EMG intensity spectra were calculated for each of 28 pedal cycles per trial where each cycle started with the left crank at top-dead-center. The total EMG intensity and the EMG intensity spectra were sub-divided into 100 equally spaced time windows. The EMG intensities for each muscle and subject were normalized to the mean of the total intensities for all spectra across all trials.

At each time window, a pattern of activity was defined as the normalized total intensities for the 10 muscles. The dominant patterns of activity were determined by principal component, PC, analysis based on a previous study (Wakeling and Rozitis 2004). Data were arranged into a $P \times N$ matrix **A**, where $P = 10$ muscles per pattern, and $n = 680{,}400$ time points analyzed (9 subjects × 9 conditions × 3 blocks × 28 pedal cycles per trial × 100 time windows per cycle). The covariance matrix **B** was calculated from the data **A**, and the PC weightings determined from the eigenvectors ζ of covariance matrix **B**. The importance of each PC was given by the eigenvalue for each eigenvalue-eigenvector pair with the greatest absolute eigenvalues corresponding to the most principal PCs. The relative proportion of the EMG patterns explained by each PC was given by $\zeta'\mathbf{B}\,\zeta$ and the loading scores for each PC for the N time points were given by $\zeta'\mathbf{A}$. Each instantaneous pattern of activity can be reconstructed from the vector product of the PC weightings and the PC loading scores. The PCs were further expressed using the varimax rotation on a subspace of the muscle activity patterns (Kaiser 1958) to simplify their visual interpretation. The subspace was defined as the space covered by the first six PCs to span the six muscle synergies previously predicted for forward pedalling (Raasch and Zajac 1999). These simplified patterns were termed varimax patterns after the PCs had been transformed with the varimax rotation.

The patterns of activity within the anatomic groups of muscles (Sol-MG-LG, VM-RF-VL, and BF-ST) were additionally determined by repeating the PC analysis using $P = 2$ or 3 corresponding to whether each anatomic group had two or three muscles, respectively.

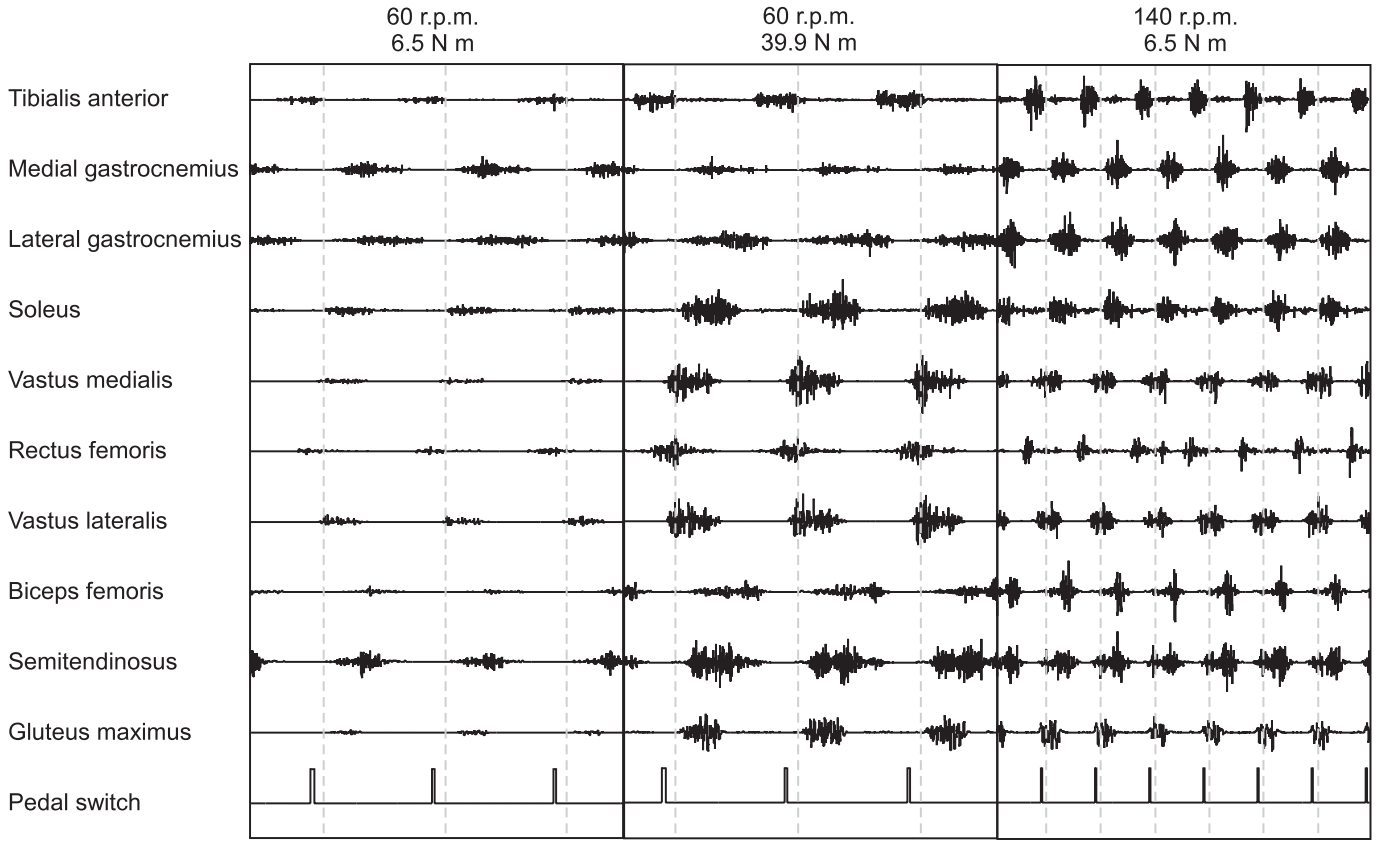

FIG. 1. Excerpts of raw electromyographic (EMG) traces from 1 subject from 3 conditions. Each panel shows 3 s of activity. Gray dashed lines show the time of the left crank at top-dead-center. The scale is the same for each muscle across the 3 conditions.

Downloaded from http://jn.physiology.org/ by 10.220.33.3 on November 11, 2017

To determine the EMG intensities at different spectral frequencies, the EMG intensities were additionally calculated for specific high- and low-frequency bands. This process is similar in concept to previous studies where the intensity has been summed across specific groups of wavelets to yield high- and low-frequency bands (Mündermann et al. 2006; Wakeling et al. 2002b); however, in this study, we specifically tuned the analysis to each muscle by calculating two specific frequency bands that explain the majority of the signal (Hodson-Tole and Wakeling 2007). In brief, PCs for the EMG intensity spectra for each muscle were calculated from the covariance matrices of the matrices of EMG intensity spectra for each muscle and subject (Wakeling and Rozitis 2004). The PCs were calculated with no prior subtraction of the mean data and describe the components of the entire signal (Wakeling and Rozitis 2004). Two intensity spectra $i(f)$ were calculated from linear combinations of the first two PCs that generated positive intensities at all frequencies and yielded the highest and lowest mean frequencies. Two wavelets were constructed to describe these spectra

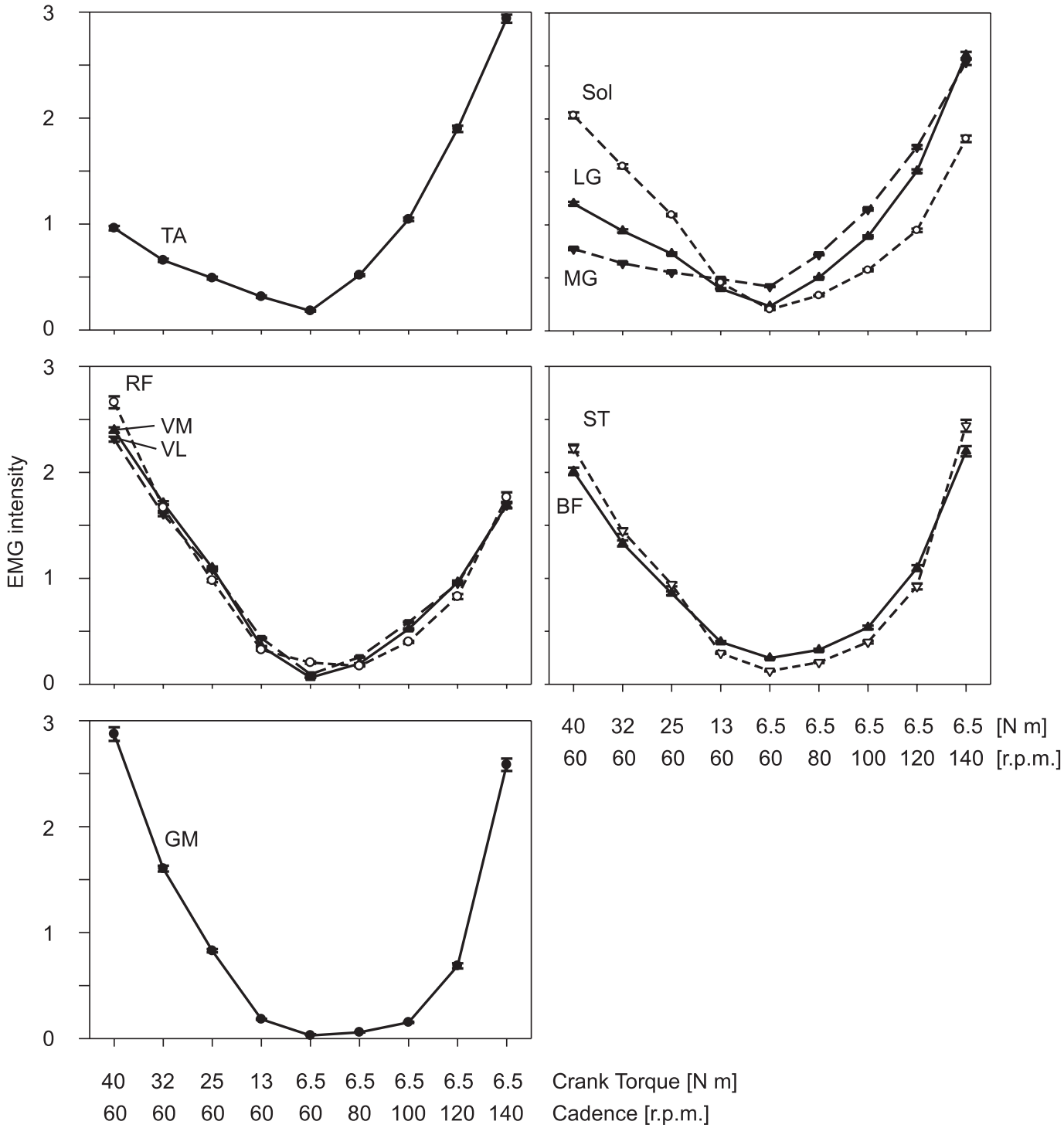

FIG. 2. Mean EMG intensity per pedal revolution as a function of crank torque and pedal cadence. Each point shows the mean ± SE (n = 756, covering all subjects, conditions and pedal revolutions).

Downloaded from http://jn.physiology.org/ by 10.220.33.3 on November 11, 2017

using least-squares minimization of a wavelet function $\psi(f)$ to $i(f)$ (Hodson-Tole and Wakeling 2007)

$$\psi(f) = \left(\frac{f}{f_c}\right)^{f_c s} e^{\left(\frac{-f}{f_c}+1\right)^{f_c s}},$$

where f_c is the center frequency of the wavelet and s is a scaling factor describing the width and shape (von Tscharner 2000). The two defined wavelets were termed $\psi_h(f)$ and $\psi_l(f)$ for high- and low-frequency bands, respectively. The EMG intensities were calculated for ψ_h and ψ_l and in a similar manner to the initial wavelet analysis (von Tscharner 2000). Each measured EMG intensity spectrum $i(f)$ was represented by the linear combination of the optimized wavelets ψ_h and ψ_l and their loading scores C_h and C_l, using nonnegative factorisation (Hodson-Tole and Wakeling 2007)

$$i(f) = C_h\psi_h(f) + C_l\psi_l(f)$$

C_h and C_l were calculated for each time point to give the time-varying $C_h(t)$ and $C_l(t)$ and were then normalized for each muscle and subject to the mean of $C_h(t) + C_l(t)$ at each time point for all trials.

To assess whether the work load was low enough not to induce fatigue, the effect of the protocol block was determined on the mean heart rate during each trial. This was assessed using a multivariate analysis of covariance of the heart rates using the following factors: subject (random), block number, and crank power; the crank power

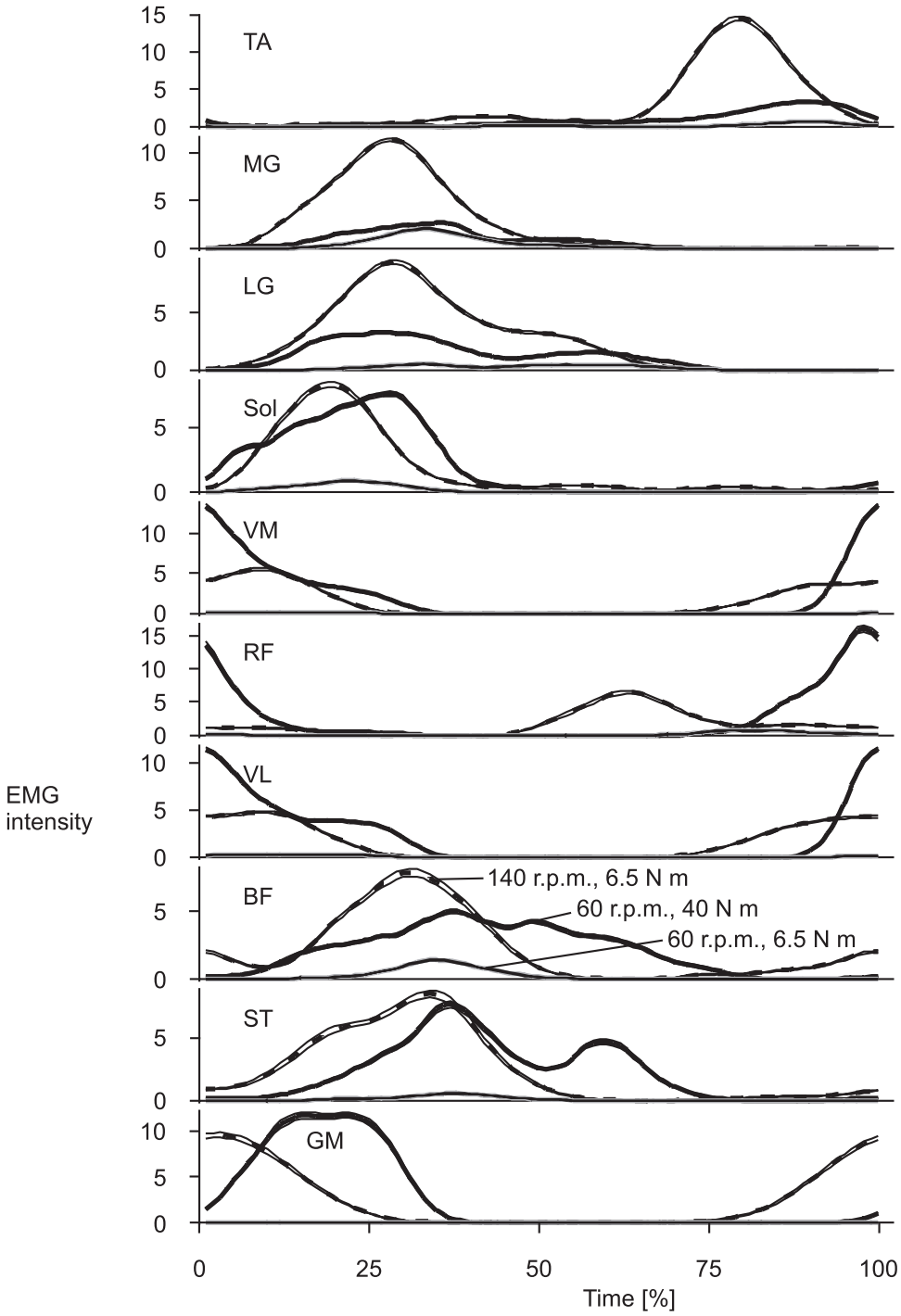

FIG. 3. Total EMG intensity during each pedal cycle for the different muscles. *Time 0* indicates the pedal at top-dead-center. Each trace shows the mean (thick line) ± SE (thin lines; $n = 756$). Gray line, data for the trials at 60 r.p.m. and 6.5 N m crank torque; solid black lines, 60 r.p.m. and 40 N m; dashed black lines, 140 r.p.m. and 6.5 N m.

Downloaded from http://jn.physiology.org/ by 10.220.33.3 on November 11, 2017

was included as a covariate. To assess whether the muscle activity patterns were associated with crank torque or pedal cadence, the effect of these parameters on the PC loading scores was tested using multivariate analysis of covariance using the following factors: subject (random), time window within pedal cycle, pedal cadence (covariate), and crank torque (covariate). EMG analyses (wavelet, PC, and varimax rotation) were carried out using Mathematica 6 software, Wolfram Research, Champaign, IL). Statistical analyses were processed using Minitab version 14 (Minitab Inc., State College, PA). All data are presented as means ± SE, and statistical tests were deemed significant at $\alpha = 0.05$.

RESULTS

The heart rate during the trials showed a significant correlation with the mechanical power output, but there was no significant difference in heart rate between the three blocks of the protocol.

The raw EMG showed that each muscle had phasic activity (Fig. 1) that varied in timing and amplitude. The patterns of muscle activity varied with both crank torque and pedal cadence. The mean EMG intensities per pedal revolution are shown in Fig. 2. All muscles showed the least mean EMG intensity for the condition with lowest mechanical power output (60 rpm and 6.5 N m). The mean EMG intensities increased with both increases in crank torque and with increases in pedal cadence. The way in which the mean EMG intensity varied with the mechanical demands differed between muscles. The TA showed greatest increases in mean EMG intensity with increased pedal cadence. The ankle extensor muscles showed different functions with the Sol being used more for the higher crank torque and the LG and MG used more for the higher cadence tasks. The MG was used less for the high torque tasks than the LG. The knee extensors showed similar patterns of mean EMG intensity except for at the highest crank torque where the RF showed greater activity than the VM and VL. From within the hamstring muscles, the ST showed a greater dynamic range across the conditions than the BF. The GM showed the greatest dynamic range of any muscle tested, and this reflected the fact that very little GM activity occurred for the low power-output tasks.

The EMG intensities, when pooled across all subjects, showed phasic patterns of activity in a similar manner to the raw traces (Fig. 3). For the ankle extensors, the maximum EMG intensity was greater for the high cadence trials for the MG and LG, but similar between the high cadence and high torque trials for the soleus. The Sol showed a pronounced shift in timing with activity being earlier for the higher cadence trials (≤9% of a pedal cycle; Figs. 3 and 4). Within the quadriceps, the RF showed a pronounced phase advance for the high cadence trials so that it was asynchronous to the VM and VL at 140 rpm and 6.5 N m, but the timing of the three muscles was much more closely matched at the 60 rpm and 40 N m trials (Fig. 3). The EMG intensity profiles showed that the BF had a much greater (57% increase) maximum intensity at the 140 rpm and 6.5 N m trial than for 60 rpm and 40 N m trial, whereas the ST was much more similar (11% increase) be-

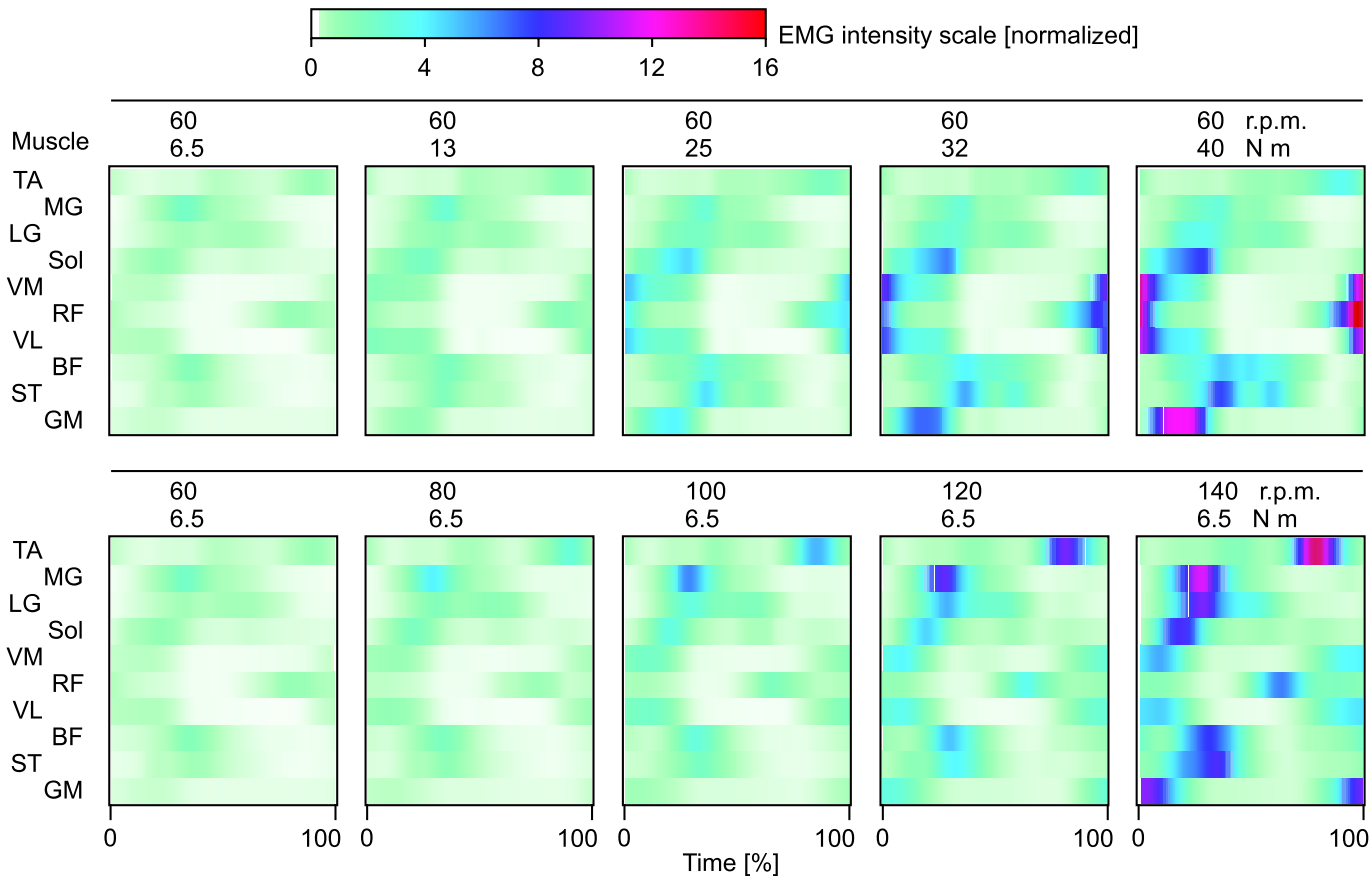

FIG. 4. EMG intensities for the different mechanical tasks. Data are the mean from all trials and all subjects. Times are normalized to a pedal revolution with *time 0* denoting the top-dead-center position for the crank.

Downloaded from http://jn.physiology.org/ by 10.220.33.3 on November 11, 2017

tween the mechanical extremes (Fig. 3). Both these hamstrings showed a relatively greater phase advance for the higher cadence trials, and the ST showed a pronounced second peak of EMG intensity (60% pedal cycle) for 60 rpm and 40 N m that did not occur for the higher cadence trials. The GM showed a pronounced phase advance at the faster cadences (Figs. 3 and 4).

The patterns of activation between the muscles can be determined from the PC analysis of the patterns of their time-varying EMG intensities (Fig. 5). More than 89% of the activity patterns were explained by the first six components. PC I showed a general level of activity for all muscles. PC II partitioned the muscles into anatomic groups with the triceps surae and hamstrings giving positive weightings while the TA, quadriceps, and GM gave negative weightings. The ANCOVA for the PC loading scores showed how the different PCs responded to the varied mechanical demands between the conditions. The PC loading scores showed significant covariance with pedal cadence and crank torque (Fig. 5) and additionally showed variation between subjects ($P < 0.001$). In this study, we were interested in the sources of intrasubject variability, and so once the subject effect was factored out by the ANCOVA, it was not considered further. The coefficients that quantified the covariance of the PC loading scores with pedal cadence or crank torque showed opposite signs for PC II, IV, and VI and between them these components explain 35.7% of the patterns of activity between the muscles (Fig. 5). Thus a large proportion of the patterns of activity between the muscles respond differently to the load and velocity of the cycling task, independent of the position of the pedal.

The varimax patterns showed uncoupling of activity between muscles within anatomic groups (Fig. 6). Uncoupling of activity between the two gastrocnemii and the soleus was explained by varimax pattern VI; and varimax pattern II additionally explained an uncoupling of activity between MG and LG. Activity in the two vastii VM and VL were uncoupled from that in the RF in varimax patterns III–VI. Uncoupling of activity between BF and ST was explained by varimax pattern III. The varimax patterns that explained uncoupling between different muscles within the anatomic groups occupied a total of 68.8% of the varimax pattern subspace.

The co-activation between muscles within anatomic groups explained no more than 79% of the activity patterns within those groups (Fig. 7). The second PCs showed that within the triceps surae 20.7% of the EMG intensities corresponded to an uncoupling of the soleus from the gastrocnemii, and in the quadriceps, 23.4% of the EMG intensities corresponded to an uncoupling of the RF from the VM and VL. In both these cases, these PC IIs accounted for uncoupling of one- from two-joint muscles. The third PCs explained uncoupling of the MG and LG in the triceps surae and of the VM and VL in the quadriceps; in both these muscle groups, these muscles originate from different sides of the leg. The second PC for the hamstrings showed that uncoupling of the BF long head from the ST accounted for 20.8% of the activity patterns: these are both two-joint muscles that originate from the ischial tuberosity but they insert on the tibial condyles on the opposite sides of the knee.

Coefficients that characterized the two major frequency components from the EMG intensity spectra are given in Table 1. When considered across all muscles, ψ_h had a mean center frequency of 105.1 Hz and ψ_l had a mean center frequency of 51.7 Hz. For both ψ_h and ψ_l the center frequencies of these optimized wavelets were lower for the more proximal muscles.

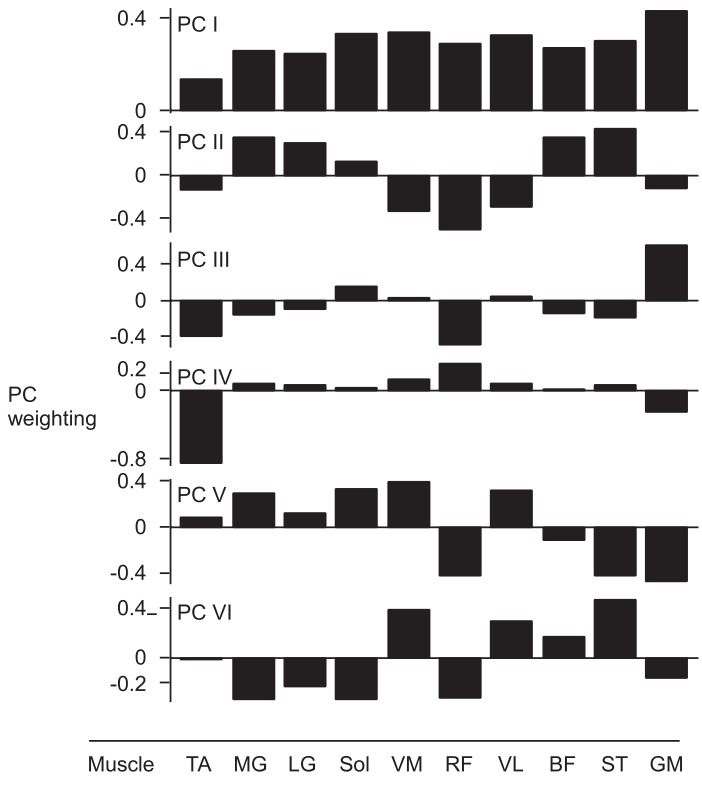

Signal [%]	Cadence [coeff.]	Torque [coeff.]
34.6	0.068	0.178
21.1	0.009	-0.024
13.3	-0.015	-0.002
9.3	-0.020	0.002
5.7	n.s.d.	-0.024
5.3	-0.003	0.019

FIG. 5. Principal component weightings for the patterns of activity among the 10 muscles calculated across all conditions. The percentage of the signal explained by each component is shown. Where the component showed a significant covariance with either pedal cadence or crank torque then the coefficient of the covariance is indicated.

Downloaded from http://jn.physiology.org/ by 10.220.33.3 on November 11, 2017

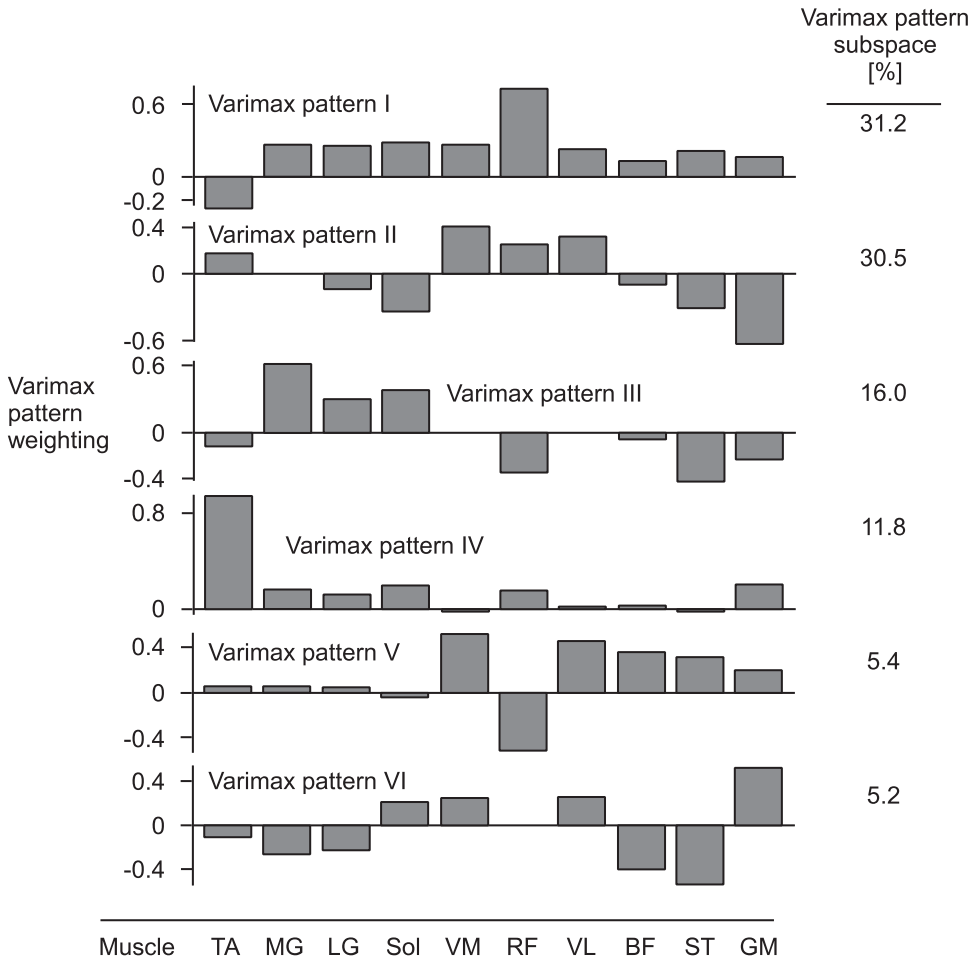

FIG. 6. Weightings of the varimax patterns from the muscle activity pattern subspace. The subspace was taken from the 1st 6 principal components shown in Fig. 5. The percentage of the subspace explained by each varimax patterns is shown.

The EMG intensities at high and low frequency bands, $C_h(t)$ and $C_l(t)$, respectively, were positively correlated for all muscles ($r = 0.978–0.997$); however, specific patterns emerged for the different muscles (Fig. 8). The EMG intensity showed a predominance for the higher frequency band for the MG and LG at the faster cadence trials. The quadriceps muscles showed the greatest correlations in EMG intensities between the high- and low-frequency bands ($r = 0.995–0.997$). The GM showed the lowest correlation ($r = 0.978$), and its EMG intensity showed a predominance for the higher frequency band at the higher torque trials.

DISCUSSION

There is current debate about the reliability of EMG measures to characterize activity patterns due to the variability that can occur in electrode placements. The proximity of the EMG electrodes to a muscle's innervation zone can affect features of the EMG signal (de Luca 1997), and the innervation zone can show considerable variability in its location for certain muscles (Rainoldi et al. 2004). However, normalized measures of EMG amplitude have been shown to remove the sensitivity to electrode placement for cycling-based studies (Malek et al. 2006), and such an approach has been used here to quantify the patterns of activity. We have recently used cross-correlation to shown that the cross-talk in raw EMG signal between adjacent muscles for our cycle tests has $r^2 < 0.04$ (Wakeling 2008b), and thus ≥96% of the EMG signal measured from an electrode can be ascribed to that muscle. Compartmentalization within a muscle can result in altered activity patterns from different muscle regions, and these vary with mechanical demand (Wakeling 2008b), but recording from a standard location for each subject ensures that similar anatomical compartments are compared. The PC analysis determines the dominant components of the signal, and so any unbiased, random noise will be included in the lower-order components. This study considered the major six PCs for the analysis of patterns of activity, and thus the remaining components (accounting for 11% of the EMG signal) were excluded. It is likely that any residual noise in the signals that was not filtered by the analysis techniques were contained in these excluded components.

As the pedalling cadence increased, a common response across the muscles tested was for the EMG intensity to advance to relatively earlier times within each pedal cycle: this is because the electromechanical delay represents an increasingly large fraction of the cycle duration at higher pedalling rates (Neptune et al. 1997). Studies reporting on the discrete activities from distinct muscles have shown that the relative levels of EMG activity varied between muscles in response to increased pedalling rates (Neptune et al. 1997; Wakeling et al. 2006). In this study, the response of the individual muscles to the varied mechanical demands also differed with the faster pedal cadences being associated with increases in EMG intensities for TA, MG, and LG, advances in timing for RF and GM, and changes in the duration of activity for BF and ST (Fig. 3).

Downloaded from http://jn.physiology.org/ by 10.220.33.3 on November 11, 2017

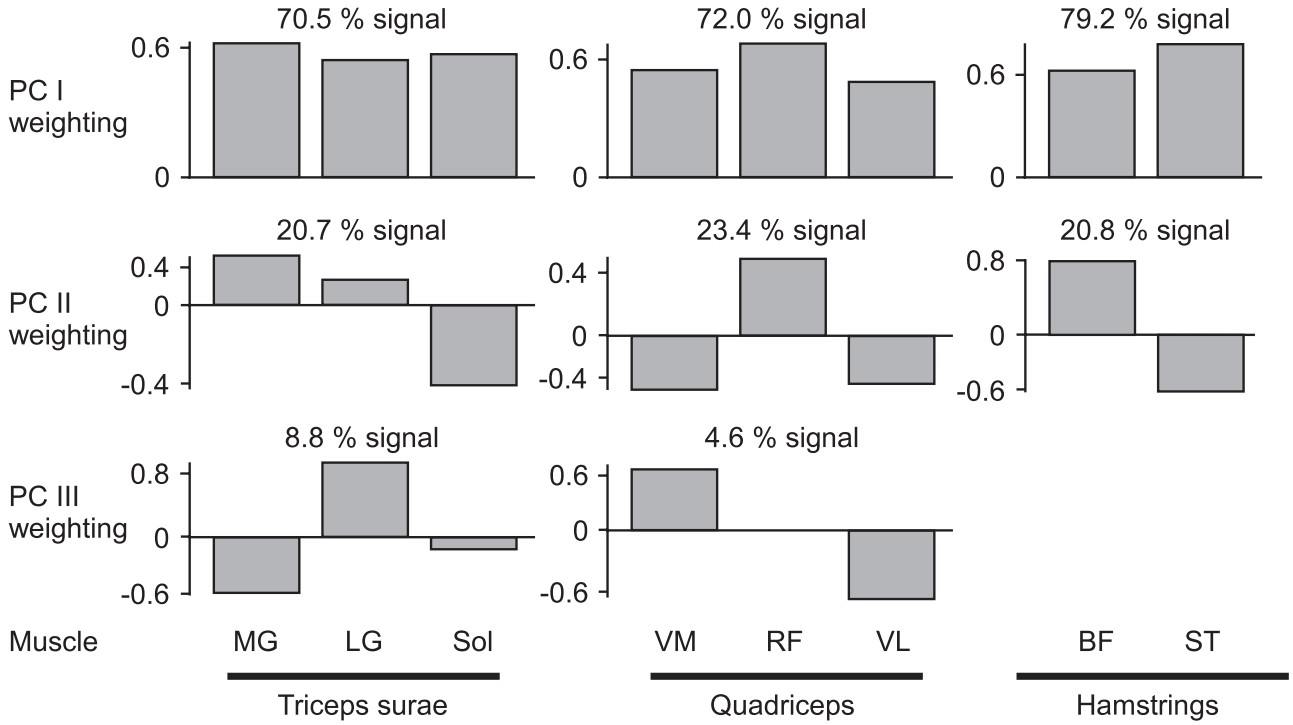

FIG. 7. Principal component weightings for the patterns of activity between the muscles in each anatomic group. The percentage of the signal explained by each component is shown.

Within each anatomic group of muscles there was evidence for uncoupling of the EMG intensities between the individual muscles: MG and LG varied in their relative EMG intensities, and both muscles varied in timing and intensity from Sol; VM and VL showed similar patterns of EMG intensity, and neither showed the pronounced phase advance for faster cadences seen in RF; BF and ST varied in their relative EMG intensities and the shape of the EMG intensity profiles (Fig. 3). Such variations between muscles within anatomic groups accounted for 68.8% of the varimax patterns (Fig. 6) and 20–30% of signals when considered in individual anatomic groups (Fig. 7). The data thus clearly support both hypotheses that a significant proportion of the patterns of activity between the leg muscles are modulated due to the movement mechanics and that activity patterns between muscles within anatomic groups show significant uncoupling when the limb is challenged with a range of mechanical conditions. The patterns of activation of individual muscles within the synergies are thus clearly modulated in association with the mechanical demands on the limb.

TABLE 1. *Coefficients that characterizes the two major frequency components from the electromyographic intensity spectra*

	ψ_l		ψ_h	
Muscle	f_c	s	f_c	s
TA	70.78 ± 9.04	0.153 ± 0.017	118.75 ± 7.08	0.142 ± 0.010
MG	74.80 ± 10.2	0.099 ± 0.020	173.00 ± 13.40	0.084 ± 0.011
LG	60.54 ± 5.46	0.126 ± 0.013	132.90 ± 11.20	0.096 ± 0.010
Sol	64.91 ± 2.59	0.142 ± 0.018	124.72 ± 6.55	0.137 ± 0.017
VM	52.78 ± 1.76	0.188 ± 0.011	97.87 ± 1.97	0.181 ± 0.012
RF	41.49 ± 2.65	0.160 ± 0.016	82.64 ± 4.83	0.174 ± 0.022
VL	44.45 ± 3.35	0.211 ± 0.012	82.85 ± 5.10	0.206 ± 0.019
BF	47.56 ± 3.64	0.116 ± 0.011	110.41 ± 6.76	0.099 ± 0.011
ST	36.69 ± 2.20	0.172 ± 0.012	77.8 ± 3.32	0.156 ± 0.017
GM	23.44 ± 1.93	0.413 ± 0.070	50.3 ± 3.36	0.202 ± 0.029

Center frequency f_c and scale s for the wavelets optimised to the low- and high-frequency components of the electromyographic (EMG) intensity from the different muscles. Values show means ± SE (n = 9 subjects). TA, tibialis anterior; MG, medial gastrocnemius; LG, lateral gastrocnemius; Sol, soleus; VM, vastus medialis; RF, rectus femoris; VL, vastus lateralis; BF, biceps femoris long head; ST, semitendinosus; GM, gluteus maximus.

The patterns of activity were calculated from EMG data that were normalized to the mean across all conditions. This approach retained the information about the relative levels of activity between the conditions and thus would focus on the more demanding high-torque low-cadence and low-torque high-cadence conditions where we hypothesized that there would be differences in pattern. An alternative approach would be to normalize each pedal cycle to the mean activity across all the muscles for that cycle: this would remove information about the relative levels of activity between conditions but would place an equal weight on the less-demanding conditions where there was less variation in mechanical demand. When tested, this alternate approach resulted in similar patterns of activity and the same conclusions regarding the uncoupling of activity within anatomic groups and modulations of the patterns of activity with crank torque and pedal cadence. Thus the patterns of activity identified in this study were relatively insensitive to the overall levels of muscle activity, and the conclusions were robust with regard to the normalization approach used.

It is not clear what factors cause the modulation of activity between some of the muscle synergies although evidence from the cat demonstrates that the some of the necessary information encoding limb velocity is present in the spinocerebellar tract (Poppele et al. 2002). Simulation studies have shown that within the triceps surae group the uniarticular Sol and biarticular MG and LG muscles act primarily with the same function

Downloaded from http://jn.physiology.org/ by 10.220.33.3 on November 11, 2017

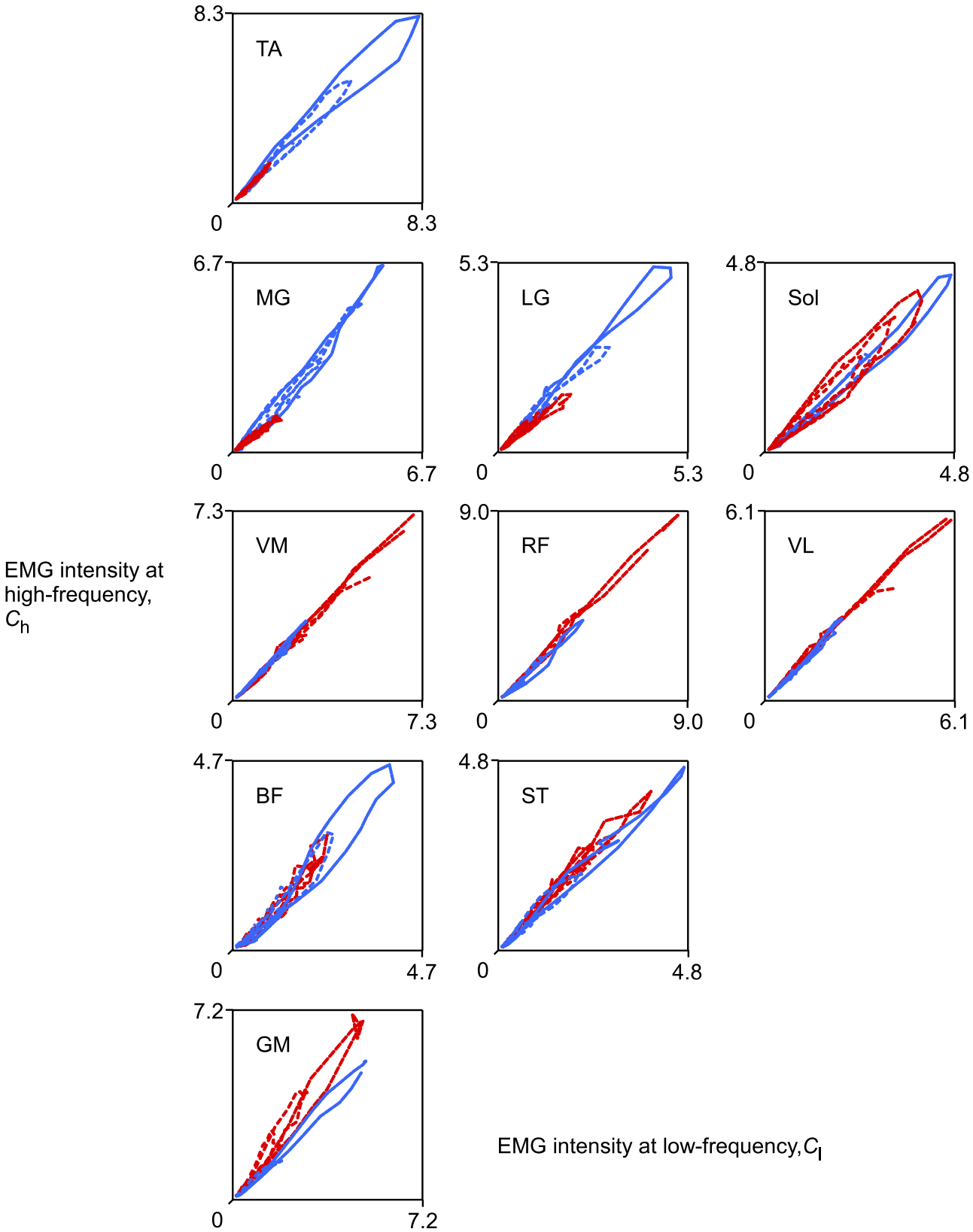

FIG. 8. Principal component loading scores C_h and C_l for all pedal conditions. The lines show the mean trajectory of the time varying loading scores for all subjects. Trials at a crank torque of 6.5 N m, but increasing cadence are shown in blue. Trials at a cadence of 60 r.p.m., but increasing crank torque are shown in red. The length of the dashes correlates to the mechanical power output for each trial.

Downloaded from http://jn.physiology.org/ by 10.220.33.3 on November 11, 2017

during cycling: stiffening the ankle and generating a tangential force on the crank (Zajac et al. 2002). The relatively greater involvement of the gastrocnemii to faster pedal cycles relative to Sol may be driven by differences in fiber type (Johnston et al. 1973) or architecture (Lieber and Fridén 2000; Wickiewicz et al. 1973) between these muscles; this supports previous observations for cycling (Wakeling et al. 2006). Furthermore, it has been shown that the faster motor units within the MG are preferentially recruited for faster cadences (Wakeling et al. 2006), highlighting the importance of muscle fiber type to the muscle recruitment. Within the quadriceps the differences in muscle fiber type and architecture among VM, RF, and VL are less pronounced (Johnston et al. 1973; Wickiewicz et al. 1973). All three muscles cross the knee joint where they act as extensors, however, the RF additionally crosses the hip. A study of the functions of these muscles, based on their EMG signals, concluded that the VM and VL were used more for the extensor phase of the pedal cycle with the RF being used more for the flexor and top-transition regions of the crank (Neptune et al. 1997; positions defined by Raasch et al. 1997). The relative changes in EMG intensity and timing between these muscles may reflect their varied mechanical roles during the pedal cycle. The BF long head and SM are both biarticular muscles originating on the ischial tuberosity and inserting on the tibial condyles, they both have long muscle fascicles and relatively high fiber to muscle length ratios (Lieber and Fridén 2000; Wickiewicz et al. 1983). Based on these architectural properties it may be assumed that these muscles act as close synergists in their activity, but this study has shown that the EMG intensity shows considerable differences in the relative intensities and timing of the EMG (Fig. 3).

Cycling studies have typically considered the pedalling motion to be kinematically constrained in the sagittal plane (Raasch and Zajac 1999; Zajac et al. 2002) and implicitly assumed that lateral forces and torques are negligible. Studies into walking around curves have shown that the relative activities of the MG and LG vary according to whether they are on the leg that is to the inside or outside of the bend; this indicates that their activity responds to the lateral forces required to negotiate the corners (Courtine et al. 2006). The lateral forces that act during cycling are not known, nor is it known how such forces vary with changing cycling mechanics. It is possible that the uncoupling of activity between MG and LG and between BF and ST (Fig. 7) is partially a response to altered lateral forces required for balance and stability during cycling; this would imply that a substantial proportion of muscle activity patterns in the leg may be required for stability rather than propulsion.

EMG signals with similar intensities but differing frequencies can indicate the activity of different task groups within the muscle (Wakeling et al. 2001). Separate bursts of myoelectric activity occur with distinct spectral properties, and these can occur within a gait cycle (von Tscharner 2000; Wakeling 2004) and vary between locomotor conditions (Wakeling 2004; Wakeling et al. 2006). Differences in the intrinsic properties of the active motor units can be inferred from the spectral content of the EMG intensities for fine-wire EMG recordings (Hodson-Tole and Wakeling 2007; Kupa et al. 1995; Wakeling and Syme 2002; Wakeling et al. 2002a). The spectral properties of the EMG are altered by volume conductor effects of the tissues, nevertheless, the differing signals from different motor units can still be distinguished using surface EMG recordings (Wakeling 2008a; Wakeling and Rozitis 2004). Both the magnitude and frequency of an EMG can change with variations in muscle temperature (Petrofsky and Lind 1980) and fatigue (Petrofsky 1979); however, in this study, the initial warm-up period followed by randomized block design of the protocol minimized such effects. Furthermore, there was no systematic increase in heart-rate during the tests illustrating that the work loads were at a low and sustainable level for these subjects. The mean frequency of the EMG may also decrease with increased muscle strain (Doud and Walsh 1995), and we have previously incorporated ultrasonic recordings of the fascicle lengths of the triceps surae muscles to show that the faster motor units are preferentially recruited for higher velocity contractions (Wakeling et al. 2006): these findings were determined by the EMG frequencies in the gastrocnemii being higher for faster pedal cadences than for higher crank torque conditions. These observations are now repeated in this study where the EMG has relatively greater intensity in the high-frequency than the low-frequency bands for the fast cycles (Fig. 8). It is interesting to note that the EMG intensity shows very little variation between the high- and low-frequency bands for the quadriceps muscles, suggesting that the recruitment patterns within these muscles have less variation than for the gastrocnemii. Furthermore, the GM shows a striking heterogeneity in the EMG intensity between the frequency bands with the faster trials resulting in a greater proportion of EMG intensity in the lower-frequency bands.

The many degrees of freedom of the musculoskeletal apparatus provide great flexibility but make the control problem extremely complex. Muscle synergies have been proposed as building blocks that could simplify the construction of motor behaviors (d'Avella et al. 2003). However, we have shown in this study that considerable variation occurs in the activity patterns between muscles within anatomic groups and that this depends on the mechanical demands of the movement task. These data indicate that the muscles of the triceps surae, the MG, LG, and Sol, may be the most responsive to the movement mechanics and in their diversity of activation patterns. We have previously reported a mechanical link between the type of motor units recruited and the mechanics of the movement task: i.e., the preferential recruitment of faster motor units at faster pedalling rates in the medial gastrocnemius in man (Wakeling et al. 2006). Motor units located in muscles from anatomic groups have been shown to share common synaptic drive during human walking (Hansen et al. 2001). It is possible that motor units that share common mechanical tasks have common patterns of activation during locomotion, and this control strategy would certainly make mechanical sense for the coordination of locomotor activities. However, some of the variations in the activation patterns that were elicited in this study appear to be directly linked to limb mechanics, muscle architecture and fiber-type composition. It is likely that the full control strategy is a complex interaction that additionally involves muscle energetics, proprioceptive afferents, and supraspinal control.

GRANTS

We thank National Sciences and Engineering Research Council for financial support for this project.

Downloaded from http://jn.physiology.org/ by 10.220.33.3 on November 11, 2017

REFERENCES

Chau T. A review of analytical techniques for gait data. I. Fuzzy, statistical and fractal methods. *Gait Posture* 13: 49–66, 2001.

Courtine G, Papaxanthis C, Schieppati M. Coordinated modulation of locomotor muscle synergies constructs straight-ahead and curvilinear walking in humans. *Exp Brain Res* 170: 320–335, 2006.

d'Avella A, Bizzi E. Shared and specific muscle synergies in natural motor behaviors. *Proc Natl Acad Sci USA* 102: 3076–3081, 2005.

d'Avella A, Saltiel P, Bizzi E. Combinations of muscle synergies in the construction of a natural motor behavior. *Nat Neurosci* 6: 300–308, 2003.

Davis BL, Vaughan CL. Phasic behavior of EMG signals during gait: use of multivariate statistics. *J Electromyogr Kinesiol* 3: 51–60, 1993.

de Luca CJ. The use of surface electromyography in biomechanics. *J Appl Biomech* 13: 135–136, 1997.

Doud JR, Walsh JM. Muscle fatigue and muscle length interaction: effect on the EMG frequency components. *Electromyogr Clin Neurophysiol* 35: 331–339, 1995.

Hansen NL, Hansen S, Christensen LO, Petersen NT, Nielsen JB. Synchronization of lower limb motor unit activity during walking in human subjects. *J Neurophysiol* 3: 1266–1276, 2001.

Hildebrand M, Goslow G. *Analysis of Vertebrate Structure* (5th ed.). New York; Wiley, 2001.

Hodson-Tole E, Wakeling JM. Variations in motor unit recruitment patterns occur within and between muscles in the running rat (*Rattus norvegicus*). *J Exp Biol* 210: 2333–2345, 2007.

Ivanenko YP, Poppele RE, Lacquaniti F. Five basic muscle activation patterns account for muscle activity during human locomotion. *J Physiol* 556: 267–282, 2004.

Johnson MA, Polgar J, Weightman D, Appleton D. Data on the distribution of fiber types in thirty-six human muscles. An autopsy study. *J Neurol Sci* 18: 111–129, 1973.

Kaiser HF. The varimax criterion for analytic rotation in factor analysis. *Psychometrika* 23: 187–200, 1958.

Kaya M, Leonard T, Herzog W. Coordination of medial gastrocnemius and soleus forces during cat locomotion. *J Exp Biol* 206: 3645–3655, 2003.

Kupa EJ, Roy SH, Kandarian SC, de Luca CJ. Effects of muscle fiber type and size on EMG median frequency and conduction velocity. *J Appl Physiol* 79: 23–32, 1995.

Lieber RL, Fridén J. Functional and clinical significance of skeletal muscle architecture. *Muscle Nerve* 11: 1647–1666, 2000.

Malek MH, Coburn JW, Weir JP, Beck TW, Housh TJ. The effects of innervation zone on electromyographic amplitude and mean power frequency during incremental cycle ergometry. *J Neurosci Methods* 155: 126–133, 2006.

Mündermann A, Wakeling JM, Nigg BM, Humble RN, Stefanyshyn DJ. Foot orthotics affect frequency components of muscle activity in the lower extremity. *Gait Posture* 23: 295–302, 2006.

Neptune RR, Kautz SA, Hull ML. The effect of pedaling rate on coordination in cycling. *J Biomech* 30: 1051–1058, 1997.

Petrofsky JS. Frequency and amplitude analysis of the EMG during exercise on the bicycle ergometer. *Eur J Appl Physiol* 41: 1–15, 1979.

Petrofsky JS, Lind AR. The influence of temperature on the amplitude and frequency components of the EMG during brief and sustained isometric contractions. *Eur J Appl Physiol* 44: 1–15, 1980.

Poppele RE, Bosco G, Rankin AM. Independent representations of limb axis length and orientation in spinocerebellar response components. *J Neurophysiol* 87: 409–422, 2002.

Raasch CC, Zajac FE. Locomotor strategy for pedaling: muscle groups and biomechanical functions. *J Neurophysiol* 82: 515–525, 1999.

Raasch CC, Zajac FE, Ma B, Levine WS. Muscle coordination during maximum-speed pedaling. *J Biomech* 30: 595–602, 1997.

Rainoldi A, Melchiorri G, Caruso I. A method for positioning electrodes during surface EMG recordings in lower limb muscles. *J Neurosci Methods* 134: 37–43, 2004.

Rome LC, Funke RP, Alexander R, McN, Lutz G, Aldridge H, Scott F, Freadman M. Why animals have different muscle fiber types. *Nature* 335: 824–827, 1988.

Smith JL, Betts B, Edgerton VR, Zernicke RF. Rapid ankle extension during paw shakes: selective recruitment of fast ankle extensors. *J Neurophysiol* 43: 612–620, 1980.

Smith JL, Spector SA. Unique contributions of slow and fast extensor muscles to the control of limb movements. *Prog Clin Neurophysiol* 9: 161–175, 1981.

Ting LH, Kautz SA, Brown DA, Zajac FE. Phase reversal of biomechanical functions and muscle activity in backwards pedaling. *J Neurophysiol* 81: 544–551, 1999.

Ting LH, Macpherson JM. A limited set of muscle synergies for force control during a postural task. *J Neurophysiol* 93: 609–613, 2005.

Tresch MC, Cheung VC, d'Avella A. Matrix factorisation algorithms for the identification of muscle synergies: evaluation on simulated and experimental data sets. *J Neurophysiol* 95: 2199–2212, 2006.

von Tscharner V. Intensity analysis in time-frequency space of surface myoelectric signals by wavelets of specified resolution. *J Electromyogr Kinesiol* 10: 433–445, 2000.

Wakeling JM. Motor units are recruited in a task-dependent fashion during locomotion. *J Exp Biol* 207: 3883–3890, 2004.

Wakeling JM. Patterns of motor recruitment can be determined using surface EMG. *J Electromyogr Kinesiol* doi:10.1016/j.jelekin.2007.09.006, 2008a.

Wakeling JM. The recruitment of different compartments within a muscle depends on the mechanics of the movement. *Biol Lett* doi:10.1098/rsbl.2008.0459, 2008b.

Wakeling JM, Kaya M, Temple GK, Johnston IA, Herzog W. Determining patterns of motor recruitment during locomotion. *J Exp Biol* 205: 359–369, 2002a.

Wakeling JM, Pascual SA, Nigg BM. Altering muscle activity in the lower extremities by running with different shoes. *Med Sci Sports Exerc* 34: 1529–1532, 2002b.

Wakeling JM, Pascual SA, Nigg BM, von Tscharner V. Surface EMG shows distinct populations of muscle activity when measured during sustained exercise. *Eur J Appl Physiol* 86: 40–47, 2001.

Wakeling JM, Rozitis AI. Spectral properties of myoelectric signals from different motor units distinguished during ramped contractions of the leg extensors. *J Exp Biol* 207: 2519–2528, 2004.

Wakeling JM, Syme DA. Wave properties of action potentials from fast and slow motor units. *Muscle Nerve* 26: 659–668, 2002.

Wakeling JM, Uehli K, Rozitis AI. Muscle fiber recruitment can respond to the mechanics of the muscle contraction. *J Roy Soc Interface* 3: 533–544, 2006.

Wickiewicz TL, Roy RR, Powell PL, Edgerton VR. Muscle architecture of the human lower limb. *Clin Orthopaed Rel Res* 179: 275–283, 1983.

Zajac FE, Neptune RR, Kautz SA. Biomechanics and muscle coordination of human walking. I. Introduction to concepts, power transfer, dynamics and simulations. *Gait Posture* 16: 215–232, 2002.

Downloaded from http://jn.physiology.org/ by 10.220.33.3 on November 11, 2017